Dynamic Inter-Modality Source Coupling Reveals Sex Differences in Children based on Brain Structural-Functional Network Connectivity: A Multimodal MRI Study of the ABCD Dataset

A. Kotoski[1,2], S-L. Wiafe[1,3], J. M. Stephen[4], Y-P. Wang[5], T. W. Wilson[6,7], and V. D. Calhoun[1]

[1] Tri-Institutional Center for Translational Research in Neuroimaging and Data Science, Atlanta, GA, USA
[2] Neuroscience Institute, Georgia State University, Atlanta, GA, USA
[3] Department of Computer Science, Georgia State University, Atlanta, GA, USA
[4] Mind Research Network, Albuquerque, NM, USA
[5] Department of Biomedical Engineering, Tulane University, New Orleans, LA, USA
[6] Institute for Human Neuroscience, Boys Town National Research Hospital, Omaha, NE, USA
[7] Department of Pharmacology and Neuroscience, Creighton University, Omaha, NE, USA

Abstract

Background: Sex differences in brain development are well-documented, yet the dynamic coupling between structure and function remains underexplored. We introduce dynamic inter-modality source coupling (dIMSC), extending our previous work to link structural MRI source-based morphometry (SBM) with dynamic functional network connectivity (dFNC).

Methods: We used data from the Adolescent Brain Cognitive Development (ABCD) study (ages 9-11) and combined SBM-derived gray matter sources with sliding-window dFNC. dIMSC was computed as the time-resolved cross-correlation between these modalities to quantify structure-function coupling strength. We evaluated sex differences in these profiles and their interaction with cognitive performance.

Results: Significant sex-specific patterns emerged: males exhibited stronger positive coupling in sensorimotor regions (postcentral gyrus), while females showed stronger coupling in higher-order associative regions (inferior parietal lobule). These configurations were functionally distinct: higher positive coupling occupancy predicted better crystallized cognition (vocabulary) in females, whereas it predicted better fluid cognition (working memory) in males.

Conclusion: Together, these findings suggest that males and females utilize distinct structural-functional configurations to support cognitive processing, males relying on a sensorimotor-anchored organization and females on an associative-anchored one. The dIMSC method advances our earlier work by enabling time-resolved analysis of brain coupling, providing a powerful framework for investigating sex-specific neurodevelopmental mechanisms.

Key words: Structure-function coupling; Sex differences; Dynamic functional connectivity; Cognition.

I. INTRODUCTION

Sex differences in brain development, historically underexamined in neuroscience, are now receiving increased attention due to their potential role in shaping cognitive, behavioral, and psychiatric trajectories [1-3]. From early childhood through adolescence, males and females exhibit differences in brain maturation rates, cortical thickness, connectivity, and functional organization [4, 5]. Prior studies have reported sex-specific patterns in brain volume, white matter development, and resting-state network activity [4, 6, 7], with some suggesting that these differences may influence emotional regulation, or susceptibility to disorders such as attention-deficit/hyperactivity disorder, anxiety, and autism [8-10]. However, while many of these findings highlight brain differences between sexes, most of the literature has examined brain structure and function in isolation, with limited insight into how brain structure-function interact across sexes during development. Therefore, the mechanisms by which coupling differ between males and females remain largely unexplored.

Structural MRI (sMRI) and resting-state functional MRI (rs-fMRI) are widely used to study the brain during development and to evaluate sex differences [4, 5]. sMRI provides information into gray and white matter anatomy, including cortical volume, thickness, and surface area [11]. Functional MRI (fMRI) is used to indirectly study the brain's activity by measuring the changes in blood-oxygen levels [12]. rs-fMRI applies this technique at rest capturing the connectivity of brain regions when no task or stimulus is being applied [13].

Prior research has demonstrated sex-related differences in both sMRI and fMRI, particularly within the developmental window of late childhood and adolescence [14-16]. Structural studies frequently report that males show larger total brain volumes, after correcting for total intracranial volume, while females exhibit accelerated maturation and achieve peak cortical volume earlier [17-19]. Regionally, females often show larger volumes in areas related to language and associative cortex [20, 21]. Resting-state studies have revealed sex differences in functional network connectivity, particularly in the default-mode network, dorsal attention network, and salience network [19]. dFNC studies have also shown sex-specific temporal characteristics, where females tend to transition more rapidly between network configurations, and males exhibit longer periods of stability within specific states [22, 23]. There is also existing work in structure-function coupling suggesting sex differences in how brain structure constrains functional connectivity in adult samples [24, 25].

To address the question of how structure-function relationship may differ by sex, it is crucial to investigate their short-term dynamic interplay. Neurobiological processes underlying development, such as synaptic pruning, myelination, and activity-dependent plasticity, are continuous and time-varying, and these processes are known to exhibit sex-specific timing [4, 15, 26, 27]. Therefore, a static, time-averaged assessment of structure-function coupling is inherently limited, as it lacks the transient periods of structural support or functional divergence that reflect these distinct sex-specific maturational events. By capturing the temporal dimension of the scan session, a dynamic approach is necessary to reveal the moments when structural constraints align with or oppose functional network activity, offering a more sensitive index of sex differences in ongoing neurodevelopmental trajectories.

In a prior study, we introduced inter-modality source coupling (IMSC) [28], a method that quantified the association between structural and functional brain components derived from independent component analysis (ICA) [29]. While IMSC has provided insights into static structure-function coupling, it does not account for temporal fluctuations that may reflect dynamic brain activity. To address this limitation, we propose a novel extension called dynamic inter-modality source coupling (dIMSC) which allows for time-resolved assessment of structure-function coupling.

The neurobiological hypothesis guiding the use of dIMSC is that functional network dynamics are not uniformly constrained by underlying structural architecture. To capture the temporal evolution of brain function, we use dynamic functional network connectivity (dFNC) derived from sliding-window based Pearson correlation, which estimates time-varying connectivity between functional brain networks [30, 31]. dFNC provides a more nuanced representation of brain activity by capturing transient brain states that are obscured when averaging over longer periods, as is done

in static FNC. Some of these dynamic states may be more closely aligned with underlying brain structure than others, making dFNC a more sensitive measure for detecting structure-function coupling. For brain structure, we utilize the source-based morphometry (SBM) components, spatially independent gray matter sources derived from ICA, to capture patterns of covarying structural variation across individuals [32]. We selected SBM over other structural modalities because fMRI signals originate within gray matter [33]. Therefore, SBM provides the direct anatomical substrate of the functional networks we are analyzing [34], allowing us to test how the structural integrity of these cortical nodes constrains their dynamic functional pattern [35]. dIMSC is computed by correlating SBM components with each temporal snapshot of dFNC pattern. We aim to explore if there is a structure-function coupling difference between males and females and investigate the functional relevance of the identified sex differences by examining whether biological sex significantly modulates the relationship between the dIMSC coupling states and a set of cognitive and behavioral measures.

II. METHODS

In this study, we use a novel method to examine time-varying interactions between brain structure and function in children aged 9–11 years-old. We analyzed baseline data from the Adolescent Brain Cognitive Development (ABCD) study, which includes over 11,000 children recruited from 21 sites across the United States. The sample is demographically diverse and was designed to approximate the U.S. population in terms of age, sex, ethnicity, and socioeconomic status [36]. This approach captures transient coupling between dynamic functional network connectivity (dFNC) and structural MRI gray matter volume. We then use it to explore sex differences in dFNC-sMRI coupling across brain regions during this critical developmental period.

A. Data

To reduce computational demand, for this project we selected a random subset of 500 unrelated individuals, matched for age, to capture meaningful effects while maintaining feasibility for analysis. The female groups consisted of 245 participants, aged between 107 months and 132 months (mean = 119 months; SD = 7 months). The male group consisted of 255 participants, aged between 107 months and 132 months (mean = 132 months; SD = 7 months). Demographic and scanner-related characteristics for each group are summarized in Table 1.

Variables	Female (n = 245)	Male (n = 255)	p value
IQ (mean ± SD)	85.86 ± 13.07	85.50 ± 10.35	0.15
MRI Scanner Site	60.3% Siemens 14.8% Philips 24.8% GE	62.0% Siemens 12.4% Philips 25.6% GE	0.52
Parental Education	18.6% high school degree or less 50.0% college degree or higher	18.5% high school degree or less 59.3% college degree or higher	0.14
Parental Employment	73.5% full-time employed	74.8% full-time employed	0.37
Household Income	19.4% low 36.4% middle 38.8% high	22.5% low 26.7% middle 45.3% high	0.58
Race/Ethnicity	57.0% White 9.1% Black or African American 33.9% other	48.4% White 12.4% Black or African American 39.2% other	0.06

Table 1. Overview of demographic and scanner-related characteristics by sex. IQ scores reflect the uncorrected NIH Toolbox total composite scores. Parental education represents the highest level of education reported by either parent, with "college degree or higher" defined as completion of a bachelor's degree, master's degree, professional degree, or doctoral degree. Parental employment indicates whether at least one parent was employed full-time. Household income was grouped into three categories, low (<$35,000), middle ($35,000-%99,999), and high (≥$100,000).

Race/ethnicity was reported by parents and categorized as White, Black or African American or Other (including Hispanic, Asian, and multiracial individuals). P-values indicate the statistical significance of differences between males and females for each category.

B. MRI Parameters

Data were collected on three types of 3T scanners (Siemens Prisma, General Electric 750 and Philips) all with a standard adult-size 32-channel head coil. The MRI sequences acquired and used for this work were a T1 structural scan (TR = 2500/2500/6.31 ms respectively; TE = 2.88/2/2.9 ms respectively). The resting-state EPI sequence used the following parameters: TR = 800 ms, TE = 30 ms, 60 slices, flip angle = 52°, matrix size = 90 × 90, FOV = 216 × 216 mm, resolution = 2.4 × 2.4 × 2.4 mm. The full details of the imaging acquisition protocol are described in [37].

C. Dynamic Inter-Modality Source Coupling

We used a standardized functional template consisting of multiple replicable resting fMRI brain networks, estimated via ICA [29], as spatial priors for both structural and functional modalities. This approach ensured consistency and comparability across subjects while also adapting to each subject individually. Specifically, we used fully automated spatially constrained ICA (scICA), applied separately to rs-fMRI and sMRI data, to extract subject-specific components while preserving spatial independence [28]. This enabled us to evaluate cross-modal coupling within a unified framework, where rs-fMRI captures individual dynamic patterns and structural brain morphometry reflects inter-subject covariation. We used the 53-component NeuroMark_fMRI_1.0 template [38] as the spatial prior, ensuring that the resulting components were both data-adaptive and comparable across modalities. All analyses were conducted using the GIFT toolbox [39].

For rs-fMRI data, we computed a dynamic functional network connectivity matrix using sliding window Pearson correlation (SWPC) [40], which estimates time-varying functional interactions. The analysis employed a rectangular window of 44s with a step size of 1 TR [30, 31], allowing us to capture fluctuations in connectivity over time. This approach provides a dynamic view of functional organization beyond static connectivity measures by characterizing how interactions between brain networks evolve temporally.

For sMRI analysis, we applied constrained SBM to estimate subject-specific loading parameters for 53 brain regions [28]. SBM is a data-driven multivariate approach that identifies spatially independent structural patterns and quantifies their expression in individual subjects [41]. Using gray matter volume as input, we extracted independent components that capture covarying patterns across subjects. Each subject's structural profile was represented by a 53-component loading vector, where each component reflects the degree to which the corresponding gray matter pattern is expressed in that individual.

To link the two modalities within our proposed dIMSC approach, we estimate the network expression coupling between the dFNC pattern and the SBM pattens via cross-correlation, computed at each time step t across 304 sliding windows between the dFNC matrix and the corresponding SBM vector for each subject:

$$dFNC(t) \in \mathbb{R}^{53X53}$$
$$SBM \in \mathbb{R}^{53X1}$$
$$dIMSC(t) = corr(dFNC(t), SBM)$$

Where:

- $dIMSC(t) \in \mathbb{R}^{53X1}$ is the dynamic inter-modality source coupling at time t for each subject.
- $dFNC(t) \in \mathbb{R}^{53X53}$ is the dynamic functional connectivity matrix at time t for each subject.
- $SBM \in \mathbb{R}^{53X1}$ is the structural component vector for each subject.

This correlation results in a timecourse that indicates how the functional characteristics of the network (represented as a column in the dFNC matrix) align with the expression of covarying gray matter components (represented as a row in the SBM mixing matrix) in each subject. This analysis resulted in a matrix that showed the degree of dynamic structure-function coupling. Figure 1 shows the pipeline for the dIMSC method. Subsequently, we categorized each timepoint based on a correlation threshold for each of the 53 brain networks based on the distribution percentiles of the dIMSC values. We selected a threshold of $\rho = \pm 0.1$, such that approximately 50% of the timepoints fall into a neutral group, while the positive and negative groups each contain approximately 25%. This distribution aligns with the expected behavior of coupling, where fluctuations around a stable mean are more common, and larger deviations occur less frequently [42]. This ensures that the positive and negative categories reflect meaningful changes in coupling while maintaining balanced subgroup sizes. On average, across all participants, 27.12% of timepoints exhibited positive coupling, 46.62% were classified as neutral, and 26.26% displayed negative coupling. For each category of the degree of time-resolved (or dynamic) structure-function coupling values, we computed the occupancy rate, representing the proportion of time a network spends in a particular coupling state.

The neutral category correlation values near zero represents timepoints where the dynamic inter-modality structure-function coupling is weak. Importantly, this category should not be interpreted as a distinct or meaningful coupling state, but rather as reflecting a stable period without significant alignment between structural and functional patterns. It serves as a reference against which deviations towards stronger positive or negative coupling can be identified or characterized. By distinguishing these neutral timepoints, we can better capture meaningful fluctuations in coupling dynamics while accounting for period of relative stability.

$$C_i(t) = \begin{cases} Positive & if\ dIMSC(t) > 0.1 \\ Neutral & if -0.1 \leq dIMSC(t) \leq 0.1 \\ Negative & dIMSC(t) < -0.1 \end{cases}$$

$$OR_{i,c} = \frac{\sum_{t=1}^{T} 1(C_i(t) = c)}{T}$$

where:

- $OR_{i,c}$ is the occupancy rate for category c in brain network i.
- T is the total number of timepoints.
- $1(C_i(t) = c)$ is an indicator function that equals 1 if $C_i(t)$ is in category c and 0 otherwise.

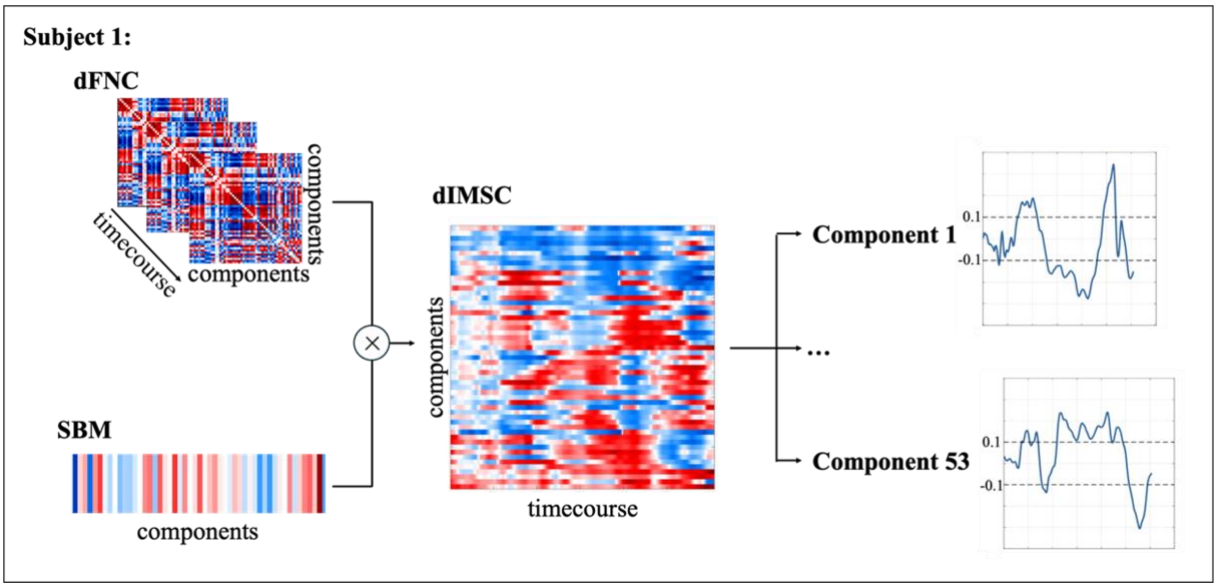

Figure 2. Overview of the dIMSC pipeline for a representative subject. The NeuroMark functional template was used as a prior in constrained ICA applied to resting-state fMRI and structural MRI data to extract 53 subject-specific functional and structural components. For rs-fMRI, a sliding window-based Pearson correlation was used to compute dFNC matrices. For sMRI, SBM was computed to generate a structural vector with 53 components. At each timepoint, dIMSC was computed as the cross-correlation between the dFNC matrix and the SBM vector, resulting in a time-resolved vector that reflects the strength of the structure-function coupling across components. The resulting matrix was decomposed into 53 dIMSC components and each timepoint based on a correlation threshold for each of the 53 brain networks based on the distribution percentiles of the values.

To examine sex differences in dIMSC measures, we conducted a multiple linear regression including a regressor for age (in months), site, and motion (mean framewise displacement), intracranial volume computed using FreeSurfer v6.0 [43], as a nuisance regressor. A significance threshold of $p < .05$ was used, with corrections for multiple comparisons applied using the false discovery rate (FDR).

D. Sex Moderation of dIMSC-Behavior Relationships

To establish the functional relevance of the dIMSC states, we performed a moderation analysis. The objective was to determine if biological sex significantly modulates the relationship between the dIMSC occupancy rate and a set of cognitive and behavioral measures. The analysis involved testing the relationship between the state-specific occupancy rate of the 53 brain networks and a total of 27 cognitive/behavioral measures across all three coupling categories (positive, neutral, negative):

$$Behavior = \beta_0 + \beta_1 * OR_c + \beta_2 * Sex + \beta_3 * (OR_c * Sex) + \epsilon$$

Where OR_c is the occupancy rate in category c (positive, neutral, negative). Sex is a binary value (male or female), and β_3 is the coefficient for the interaction term $(OR_c * Sex)$, indicating that biological sex moderated the relationship. The model also included the following covariates: age (in months), site, intracranial volume, and motion (mean framewise displacement). A significance threshold of $p < 0.05$ was used, with corrections for multiple comparisons applied across all 53 networks, 3 coupling states, and 27 behavioral measures using false discovery rate.

We utilized a total of 27 measures spanning executive function, language, reading, fluid/crystallized cognition, and memory from the NIH Toolbox and the Rey Auditory Verbal Learning Test (RAVLT). The specific measures included in the moderation analysis were:

1. NIH Toolbox Executive Function:
    - Flanker Inhibitory Control and Attention: Uncorrected and age-corrected scores
    - List Sorting Working Memory: Uncorrected and age-corrected scores
    - Dimensional Change Card Sort: Uncorrected and age-corrected scores
    - Pattern Comparison Processing Speed: Uncorrected and age-corrected scores
2. NIH Toolbox Language & Reading:
    - Picture Vocabulary: Uncorrected score, age-corrected score, and T-score
    - Picture Sequence Memory: Uncorrected score, age-corrected score, and T-score
    - Oral Reading Recognition: Uncorrected score, age-corrected score, and T-score
3. NIH Toolbox Composite Scores:
    - Fluid Cognition Composite: Uncorrected and age-corrected scores
    - Crystallized Cognition Composite: Uncorrected and age-corrected scores
    - Total Cognition Composite: Uncorrected and age-corrected scores
4. RAVLT Memory Measures:
    - RAVLT Immediate Recall (Trial I-V Sum): T-score
    - RAVLT Delayed Recall (Trial VII): T-score
    - RAVLT Recognition Hits (Trial VI): T-score
    - RAVLT Semantic/Category Recall (List B Interference): T-score

III. RESULTS

The application of dIMSC revealed distinct temporal patterns of structure-function coupling across the 53 brain networks. By estimating the coupling between the network expression of the dFNC matrix and the SBM vector at each timepoint, we obtained a time-resolved measure of coupling strength. These values were grouped into three categories: positive, neutral, and negative coupling. Specifically, positive coupling indicates that increases in structural properties are associated with increases in functional properties, suggesting a coordinated relationship; neutral coupling indicates that structural and functional properties are relatively independent of each other; and negative coupling implies an inverse relationship, potentially indicating compensatory or opposing mechanisms between the areas.

The mean coupling strength was 0.18 ± 0.04 for positive states, 0.0001 ± 0.02 for neutral states, and -0.17 ± 0.04 for negative states. This distribution indicates a predominant trend of balanced structure-function alignment across the sample, with stronger positive and negative coupling suggesting a bidirectional relationship between structural and functional features in specific networks. When analyzed separately by sex, males exhibited positive coupling in 26.96% of timepoints, neutral coupling in 47.16%, and negative coupling in 25.89%. The corresponding mean coupling strengths were 0.18 ± 0.04 for positive states, 0.0002 ± 0.02 for neutral states, and -0.17 ± 0.04 for negative states. In females, positive coupling was observed in 27.30% of timepoints, neutral coupling in 46.08%, and negative coupling in 26.63%, with mean coupling strengths of 0.17 ± 0.04, $5.43 \times 10^{-6} \pm 0.02$, and -0.17 ± 0.04, respectively. These results indicate that males showed a slightly higher proportion of timepoints with neutral coupling, while females exhibited a marginally greater proportion of negative and positive coupling. Figure 2 illustrates the distribution of the coupling for males and females. On average, males had a total intracranial volume of 1583.55 ± 119.96 cm³, while females had an average intracranial volume of 1438.48 ± 191.21 cm³. To account for potential head size effects, all statistical comparisons were adjusted for intracranial volume.

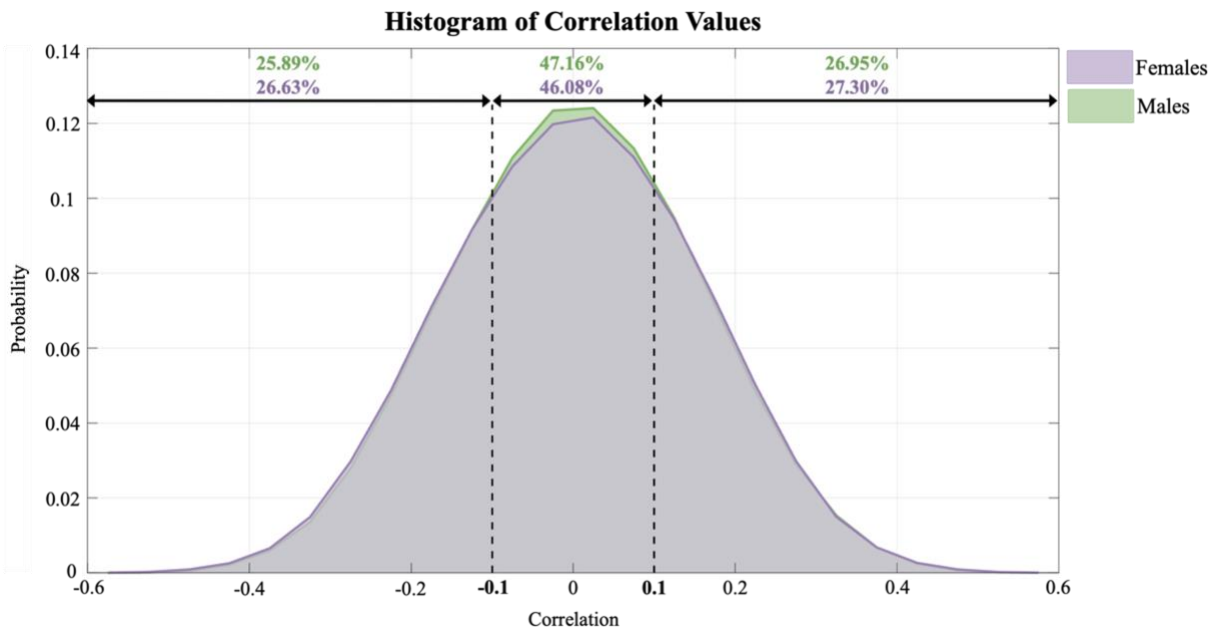

Figure 2. This histogram displays the distribution of coupling for males (on the back, shown in green), and females (on the front, shown in purple). The x-axis represents the correlation value between structure and function, while the y-axis indicates the probability of distributions. Vertical dashed lines are placed at -0.1 and 0.1 along the x-axis to define the three categories: negative, neutral and positive. These thresholds highlight a clear group-level difference, where around 50% of the values are concentrated in the neutral group. For the females, this distribution suggests a greater proportion of negative and positive values when compared to males. In contrast, the male's correlation values are more centered around the neutral group, indicating that males tend to exhibit more neutral values on this coupling.

Sex differences in dIMSC were observed across several brain networks. Figure 3 provides spatial brain maps highlighting the identified regions, while Figure 4 presents the occupancy rate values for significant brain regions in both males and females. Within the positive coupling category, females exhibited stronger coupling in the inferior parietal lobule and precuneus compared to males, suggesting enhanced structural support for functional activity in these regions. In the neutral coupling category, males demonstrated stronger coupling in the cerebellum and superior temporal gyrus, while females exhibited stronger coupling in the caudate, precentral, and middle frontal gyrus, suggesting that different brain regions may underlie sex-specific structure-function coupling during this state. For the negative coupling category, males showed stronger coupling in the paracentral lobule, superior parietal lobule, and middle temporal gyrus, while females exhibited stronger coupling in the superior temporal gyrus ad inferior parietal lobule.

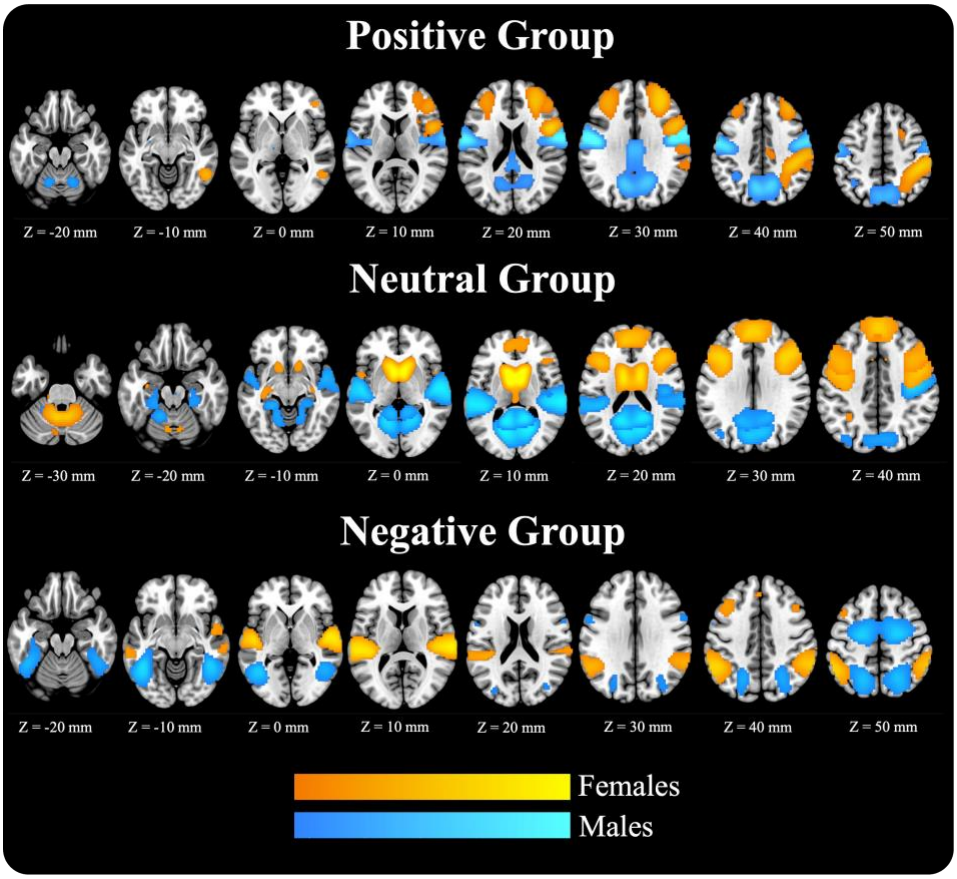

Figure 3. Brain maps showing significant sex differences in structure-function coupling across categories. Regions with significant group differences are displayed separately for positive group (top), neutral group (middle), and negative (bottom). Males are shown in blue and females in orange, allowing for visual comparison between categories. Anatomical localization is shown in MNI space.

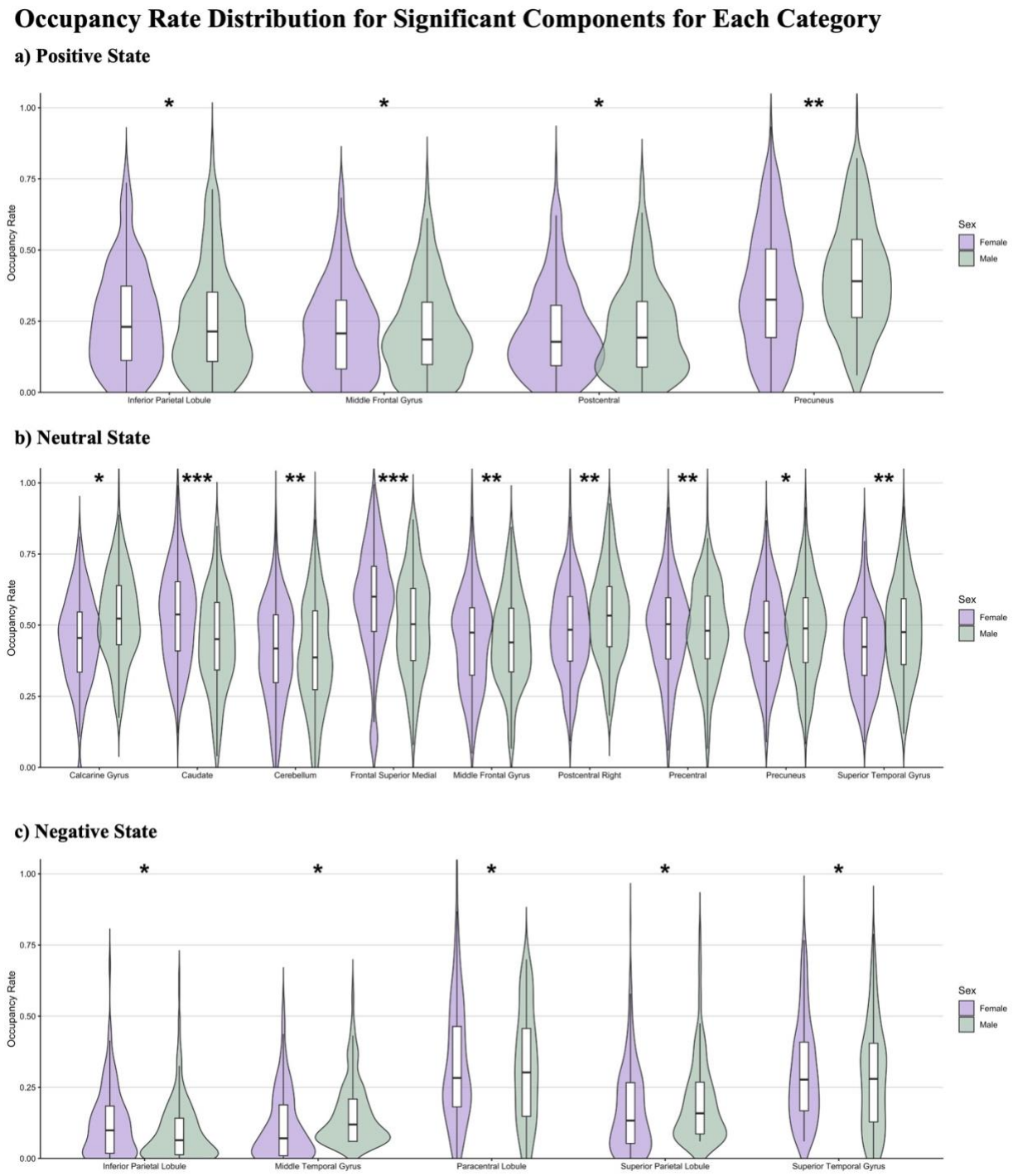

Figure 4. Category-level violin plots displaying state-specific occupancy rates for brain regions that exhibited significant sex differences, with values shown separately for males (green) and females (purple). The y-axis represents the occupancy rate, defined as the proportion of timepoints during which each brain region was classified within a specific coupling state. The x-axis lists the individual brain regions for each group. Asterisks indicate statistically significant group differences (* for $0.05 > p > 0.01$, ** for $0.01 > p > 0.001$, and *** for $p < 0\ .001$), corrected for multiple comparisons using FDR. Notably, sex differences appear relatively evenly distributed across all three coupling states. This suggests that sex differences in brain activity patterns occur throughout the full range of brain

network dynamics. This pattern might reflect that biological sex influences the coordinated brain activity in general, regardless of the specific coupling strength.

The moderation analysis, which tested the sex and dIMSC interaction on 27 cognitive and behavioral measures, revealed numerous significant findings across all three coupling categories (positive, neutral, and negative). These results demonstrate that the relationship between the time a brain network spends in a specific dIMSC state and cognitive performance is significantly modulated by biological sex. The beta coefficients for the significant interaction terms are summarized in the heatmaps (Figure 5).

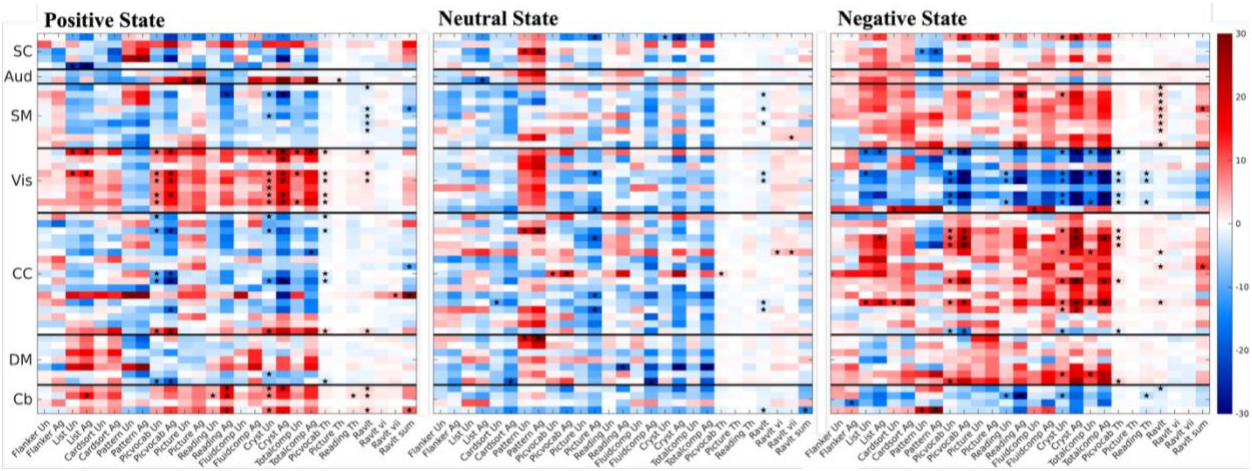

Figure 5. This figure displays the β_3 coefficients from the moderation analysis. Each panel shows the interactions for a different dIMSC coupling states (positive, neutral, or negative). The y-axis represents the 53 brain networks components, grouped by domains (SC: subcortical, Aud: auditory, SM: sensorimotor, Vis: Visual, CC: cognitive control, DM: default mode, Cb: cerebellum). The x-axis lists the 27 behavioral and cognitive measures. The color scales indicate the direction of the interaction effect: red (positive coefficients) signifies that the association between dIMSC and cognitive performance is stronger in females than males (F>M). Blue (negative coefficients) signifies that the association is stronger in males than females (M>F). The stars denote statistically significant interactions after FDR correction ($p < .05$).

The positive coupling state, which reflects strong structural-functional alignment, exhibited significant and distinct sex-specific associations with cognition. We observed female-dominant interactions where higher occupancy in the positive state was more strongly associated with better performance in females, particularly for crystallized cognition measures. These interactions were centered in regions including the thalamus, calcarine sulcus, cerebellum, and other areas of the visual cortex. Conversely, males exhibited stronger reliance on the positive coupling state for better performance across measures of executive function and working memory. These male-dominant interactions involved the thalamus, cerebellum, calcarine sulcus, hippocampus, postcentral, and paracentral gyri. The thalamus emerged as a central hub for interactions across multiple measures.

The neutral coupling state, characterized by weak structure-function alignment, also demonstrated significant moderation effects, with almost all interactions for working memory and fluid reasoning being associated with males. For executive function, interactions were mixed; while some were evident in males, such as the card sort test, interactions related to pattern comparison processing speed were generally more pronounced in females. The prevalent M>F pattern for working memory and fluid reasoning suggests that males exhibit a more widespread dependence on certain areas to predict their cognitive performance, even when the dIMSC coupling is weak. This may reflect a reliance on more robust neural networks in males when structural-functional alignment is relatively low.

The negative coupling state, representing an inverse relationship between structure and function, showed strong, widespread interactions, often stronger in females. Significant interactions in females were observed across multiple domains, including working memory and fluid reasoning, involving sensorimotor and attentional networks such as

the postcentral and paracentral gyri, inferior parietal lobule, cerebellum, and superior parietal lobule. Strong female interactions were also found in language-related areas and memory/visual areas for verbal and crystallized cognition, while stronger male interactions were present in frontal superior areas.

IV. DISCUSSION

In this study, we introduced dynamic inter-modality source coupling, a novel method to quantify the time-varying constraints that brain structure imposes on functional dynamics. Extending our previous IMSC method [28], dIMSC moves beyond the assumption that structure-function relationships are constant, instead modeling them as fluctuating states of alignment (positive), independence (neutral), or divergence (negative). By applying this framework to a large sample of children from the ABCD study, we demonstrate that the coupling between gray matter architecture and functional connectivity is not uniform but state-dependent, and the organization of these states exhibits significant sex differences that are relevant to cognitive performance.

The classification of coupling into positive, neutral, and negative states provides a theoretical framework for interpreting neurodevelopmental dynamics. Positive coupling reflects periods where functional connectivity patterns tightly align with the underlying structural scaffold, a state consistent with the “structural constraint” hypothesis where anatomy constrains function [44, 45]. Neutral coupling, which comprised the largest proportion of timepoints, suggests periods where functional dynamics operate independently of the specific structural priors used here, potentially reflecting flexible, polysynaptic signaling that transcends direct anatomical links [24]. Negative coupling, representing an inverse relationship, likely reflects a state of functional divergence or segregation, where functional networks actively decouple from their structural basis to support complex, transient cognitive states [25]. The balance between these states and how they differ by sex offers a new window into the maturation of the adolescent brain.

We observed a robust dissociation in which males and females exhibit strong structure-function alignment (positive coupling). Females showed significantly stronger positive coupling in higher-order associative regions, specifically the inferior parietal lobule (IPL) and middle frontal gyrus (MFG). This finding aligns with established literature indicating that females often reach developmental peaks in cortical volume earlier than males [14, 18] and possess proportionally larger volumes in language and associative cortices [20, 21]. The stronger structural constraint in these regions suggests a more mature integration of the “social brain” and executive control networks in females at this age, consistent with their typically earlier maturation of social-cognitive skills [1, 5].

In contrast, males exhibited stronger positive coupling in sensorimotor and visuospatial regions (postcentral gyrus, precuneus). This pattern mirrors findings from adult structural connectome studies, which show that male brains are optimized for intra-hemispheric communication and sensorimotor coordination [17], while female brains facilitate inter-hemispheric communication [17]. Furthermore, recent work on structure-function coupling in adults [24] identified that males exhibit tighter coupling in "rich-club" connections (linking high-traffic hubs to each other), whereas females show stronger coupling in "feeder" connections (linking these central hubs to peripheral non-hub regions). Our results suggest these distinct organizational principles, males’ anchoring function to structure in sensorimotor systems and females’ in associative systems, are already present and detectable in late childhood.

Crucially, our moderation analysis revealed that these coupling states are differentially linked to cognition in males and females. We found that biological sex significantly modulated the relationship between dIMSC occupancy and performance, particularly in the positive coupling state. For females, higher occupancy in the positive state was associated with better performance in crystallized cognition (vocabulary, reading). These interactions were centered on the thalamus, cerebellum, and visual areas. This suggests that for females, accessing stored knowledge and verbal skills relies on a functional architecture that is tightly constrained by structural anatomy. This is consistent with the “adaptive complementarity” hypothesis [16], where female advantages in verbal memory are supported by specific structural efficiencies in temporo-parietal networks.

For males, stronger positive coupling was associated with better performance in fluid cognition, specifically executive function and working memory. These interactions involved the hippocampus and paracentral lobule. This indicates that males who are better able to align their functional dynamics with their structural scaffold in these regions perform better on tasks requiring varying processing speed and inhibition. Interestingly, in the neutral state (weak coupling), males continued to show strong brain-behavior associations for working memory, whereas females did not. This may imply that males rely on a more “hard-wired” or structurally anchored strategy for executive functioning, even when functional dynamics are less constrained, whereas females may utilize more flexible, structurally independent functional states to achieve similar cognitive goals [22, 23].

The observation that males show stronger coupling in sensorimotor systems while females show it in associative systems supports the theory that brain maturation proceeds along a sensorimotor-to-associative axis, but at different rates between sexes [46]. The “structural anchoring” seen in males may reflect a prolonged period of synaptic pruning and refinement in these lower-order networks [6], whereas the enhanced coupling in females likely reflects the earlier onset of myelination and stabilization in higher-order association cortices [4, 47, 48]. These distinct developmental trajectories underscore the importance of analyzing males and females separately in clinical studies, as the "healthy" baseline for structure-function integration differs by sex.

While dIMSC offers a powerful new metric, this study is limited by its cross-sectional nature. Longitudinal analysis is required to determine if the male-sensorimotor/female-associative difference reflects a permanent sexual dimorphism or a transient developmental phase (i.e., males eventually “catching up” in associative coupling). Additionally, while we controlled for motion and volume, future work should explore how pubertal hormones (testosterone and estradiol) specifically drive these coupling shifts, as they are known to regulate synaptic plasticity and myelination in a sex-specific manner [27, 49-51].

V. CONCLUSIONS

This study establishes dynamic inter-modality source coupling as a sensitive framework for mapping the time-varying interactions between brain structure and function. We provide evidence that the “rules” governing how function is constrained by structure differ fundamentally between sexes in childhood. Males exhibit a "sensorimotor-anchored" organization, where stronger structure-function coupling in motor and visual regions supports fluid reasoning. Females exhibit an “associative-anchored” organization, where coupling in parietal and frontal higher-order cortices supports crystallized cognition. These findings underscore the necessity of accounting for sex as a biological variable in neurodevelopmental research and demonstrate the utility of dIMSC for uncovering sex-specific mechanisms of brain organization that may be relevant for understanding heterogeneity in developmental disorders.

Funding: This work was supported in part by NIH under grants R01MH118695, R01EB036247 and P20-GM144641 and in part by NSF under grants 2112455 and 2316421.

REFERENCES

[1] D. I. Miller and D. F. Halpern, "The new science of cognitive sex differences," *Trends in cognitive sciences,* vol. 18, no. 1, pp. 37-45, 2014.

[2] P. Okami and T. K. Shackelford, "Human sex differences in sexual psychology and behavior," *Annual Review of Sex Research,* vol. 12, no. 1, pp. 186-241, 2001.

[3] D. A. Bangasser and R. J. Valentino, "Sex differences in stress-related psychiatric disorders: neurobiological perspectives," *Frontiers in neuroendocrinology,* vol. 35, no. 3, pp. 303-319, 2014.

[4] M. D. De Bellis *et al.*, "Sex differences in brain maturation during childhood and adolescence," *Cerebral cortex,* vol. 11, no. 6, pp. 552-557, 2001.

[5] G. Gong, Y. He, and A. C. Evans, "Brain connectivity: gender makes a difference," *Neuroscientist,* vol. 17, no. 5, pp. 575-91, Oct 2011, doi: 10.1177/1073858410386492.

[6] J. S. Perrin *et al.*, "Sex differences in the growth of white matter during adolescence," *Neuroimage,* vol. 45, no. 4, pp. 1055-1066, 2009.

[7] G. Alarcón, A. Cservenka, M. D. Rudolph, D. A. Fair, and B. J. Nagel, "Developmental sex differences in resting state functional connectivity of amygdala sub-regions," *Neuroimage,* vol. 115, pp. 235-244, 2015.

[8] E. K. Gardener, A. R. Carr, A. MacGregor, and K. L. Felmingham, "Sex differences and emotion regulation: an event-related potential study," *PloS one,* vol. 8, no. 10, p. e73475, 2013.

[9] L. E. Arnold, "Sex differences in ADHD: Conference summary," *Journal of abnormal child psychology,* vol. 24, pp. 555-569, 1996.

[10] S. Baron-Cohen, R. C. Knickmeyer, and M. K. Belmonte, "Sex differences in the brain: implications for explaining autism," *Science,* vol. 310, no. 5749, pp. 819-823, 2005.

[11] T. V. Phan, D. Sima, D. Smeets, P. Ghesquiere, J. Wouters, and M. Vandermosten, "Structural brain dynamics across reading development: A longitudinal MRI study from kindergarten to grade 5," *Hum Brain Mapp,* vol. 42, no. 14, pp. 4497-4509, Oct 1 2021, doi: 10.1002/hbm.25560.

[12] N. M. Correa, Y.-O. Li, T. Adali, and V. D. Calhoun, "Fusion of fMRI, sMRI, and EEG data using canonical correlation analysis," in *2009 IEEE International Conference on Acoustics, Speech and Signal Processing*, 2009: IEEE, pp. 385-388.

[13] M. H. Lee, C. D. Smyser, and J. S. Shimony, "Resting-state fMRI: a review of methods and clinical applications," *AJNR Am J Neuroradiol,* vol. 34, no. 10, pp. 1866-72, Oct 2013, doi: 10.3174/ajnr.A3263.

[14] J. N. Giedd, F. X. Castellanos, J. C. Rajapakse, A. C. Vaituzis, and J. L. Rapoport, "Sexual dimorphism of the developing human brain," *Progress in Neuro-Psychopharmacology and Biological Psychiatry,* vol. 21, no. 8, pp. 1185-1201, 1997.

[15] J. N. Giedd *et al.*, "Brain development during childhood and adolescence: a longitudinal MRI study," *Nat Neurosci,* vol. 2, no. 10, pp. 861-3, Oct 1999, doi: 10.1038/13158.

[16] T. D. Satterthwaite *et al.*, "Linked sex differences in cognition and functional connectivity in youth," *Cerebral cortex,* vol. 25, no. 9, pp. 2383-2394, 2015.

[17] M. Ingalhalikar *et al.*, "Sex differences in the structural connectome of the human brain," *Proc Natl Acad Sci U S A,* vol. 111, no. 2, pp. 823-8, Jan 14 2014, doi: 10.1073/pnas.1316909110.

[18] R. K. Lenroot and J. N. Giedd, "Sex differences in the adolescent brain," *Brain Cogn,* vol. 72, no. 1, pp. 46-55, Feb 2010, doi: 10.1016/j.bandc.2009.10.008.

[19] B. A. Shaywitz *et al.*, "Sex differences in the functional organization of the brain for language," *Nature,* vol. 373, no. 6515, pp. 607-9, Feb 16 1995, doi: 10.1038/373607a0.

[20] J. Harasty, K. L. Double, G. M. Halliday, J. J. Kril, and D. A. McRitchie, "Language-associated cortical regions are proportionally larger in the female brain," *Arch Neurol,* vol. 54, no. 2, pp. 171-6, Feb 1997, doi: 10.1001/archneur.1997.00550140045011.

[21] R. C. Gur *et al.*, "Sex differences in brain gray and white matter in healthy young adults: correlations with cognitive performance," *J Neurosci,* vol. 19, no. 10, pp. 4065-72, May 15 1999, doi: 10.1523/JNEUROSCI.19-10-04065.1999.

[22] L. Murray, J. M. Maurer, A. L. Peechatka, B. B. Frederick, R. H. Kaiser, and A. C. Janes, "Sex differences in functional network dynamics observed using coactivation pattern analysis," *Cogn Neurosci,* vol. 12, no. 3-4, pp. 120-130, Jul-Oct 2021, doi: 10.1080/17588928.2021.1880383.

[23] M. Nini, Z. Hongna, L. Zhiying, Y. Li, and W. Xia, "Gender differences in dynamic functional connectivity based on resting-state fMRI," *Annu Int Conf IEEE Eng Med Biol Soc,* vol. 2017, pp. 2940-2943, Jul 2017, doi: 10.1109/EMBC.2017.8037473.

[24] S. Zhao *et al.*, "Sex Differences in Anatomical Rich-Club and Structural-Functional Coupling in the Human Brain Network," *Cereb Cortex,* vol. 31, no. 4, pp. 1987-1997, Mar 5 2021, doi: 10.1093/cercor/bhaa335.

[25] B. Wan *et al.*, "Heritability and cross-species comparisons of human cortical functional organization asymmetry," *Elife,* vol. 11, Jul 29 2022, doi: 10.7554/eLife.77215.

[26] R. K. Lenroot and J. N. Giedd, "Brain development in children and adolescents: insights from anatomical magnetic resonance imaging," *Neurosci Biobehav Rev,* vol. 30, no. 6, pp. 718-29, 2006, doi: 10.1016/j.neubiorev.2006.06.001.

[27] C. L. Sisk and J. L. Zehr, "Pubertal hormones organize the adolescent brain and behavior," *Front Neuroendocrinol,* vol. 26, no. 3-4, pp. 163-74, Oct-Dec 2005, doi: 10.1016/j.yfrne.2005.10.003.

[28] A. Kotoski, J. Liu, R. Morris, and V. Calhoun, "Inter-Modality Source Coupling: A Fully-Automated Whole-Brain Data-Driven Structure-Function Fingerprint Shows Replicable Links to Reading in a Large-Scale (N approximately 8K) Analysis," *IEEE Trans Biomed Eng,* vol. 71, no. 12, pp. 3383-3389, Dec 2024, doi: 10.1109/TBME.2024.3423703.

[29] T.-W. Lee, "Independent component analysis," in *Independent component analysis: Theory and applications*: Springer, 1998, pp. 27-66.

[30] E. A. Allen, E. Damaraju, S. M. Plis, E. B. Erhardt, T. Eichele, and V. D. Calhoun, "Tracking whole-brain connectivity dynamics in the resting state," *Cerebral cortex,* vol. 24, no. 3, pp. 663-676, 2014.

[31] S. L. Wiafe, N. O. Asante, V. D. Calhoun, and A. Faghiri, "Studying time-resolved functional connectivity via communication theory: on the complementary nature of phase synchronization and sliding window Pearson correlation," *bioRxiv,* Nov 22 2024, doi: 10.1101/2024.06.12.598720.

[32] L. Xu, K. M. Groth, G. Pearlson, D. J. Schretlen, and V. D. Calhoun, "Source-based morphometry: the use of independent component analysis to identify gray matter differences with application to schizophrenia," *Hum Brain Mapp,* vol. 30, no. 3, pp. 711-24, Mar 2009, doi: 10.1002/hbm.20540.

[33] N. K. Logothetis, J. Pauls, M. Augath, T. Trinath, and A. Oeltermann, "Neurophysiological investigation of the basis of the fMRI signal," *Nature,* vol. 412, no. 6843, pp. 150-7, Jul 12 2001, doi: 10.1038/35084005.

[34] J. M. Segall *et al.*, "Correspondence between structure and function in the human brain at rest," (in English), *Front Neuroinform,* vol. 6, 2012, doi: ARTN 10

10.3389/fninf.2012.00010.

[35] J. Sui, R. Huster, Q. Yu, J. M. Segall, and V. D. Calhoun, "Function-structure associations of the brain: evidence from multimodal connectivity and covariance studies," *Neuroimage,* vol. 102 Pt 1, pp. 11-23, Nov 15 2014, doi: 10.1016/j.neuroimage.2013.09.044.

[36] N. D. Volkow *et al.*, "The conception of the ABCD study: From substance use to a broad NIH collaboration," *Dev Cogn Neurosci,* vol. 32, pp. 4-7, Aug 2018, doi: 10.1016/j.dcn.2017.10.002.

[37] B. J. Casey *et al.*, "The adolescent brain cognitive development (ABCD) study: imaging acquisition across 21 sites," *Developmental cognitive neuroscience,* vol. 32, pp. 43-54, 2018.

[38] Y. Du *et al.*, "NeuroMark: An automated and adaptive ICA based pipeline to identify reproducible fMRI markers of brain disorders," *Neuroimage Clin,* vol. 28, p. 102375, 2020, doi: 10.1016/j.nicl.2020.102375.

[39] V. D. Calhoun, T. Adali, G. Pearlson, and J. Pekar, "Group ICA of functional MRI data: separability, stationarity, and inference," in *Proc. Int. Conf. on ICA and BSS San Diego, CA*, 2001, vol. 155, pp. 155-160.

[40] R. Hindriks *et al.*, "Can sliding-window correlations reveal dynamic functional connectivity in resting-state fMRI?," *Neuroimage,* vol. 127, pp. 242-256, 2016.

[41] C. N. Gupta, J. A. Turner, and V. D. Calhoun, "Source-based morphometry: a decade of covarying structural brain patterns," *Brain Structure and Function,* vol. 224, no. 9, pp. 3031-3044, 2019.

[42] R. M. Hutchison, T. Womelsdorf, J. S. Gati, S. Everling, and R. S. Menon, "Resting-state networks show dynamic functional connectivity in awake humans and anesthetized macaques," *Human brain mapping,* vol. 34, no. 9, pp. 2154-2177, 2013.

[43] B. Fischl, "FreeSurfer," *Neuroimage,* vol. 62, no. 2, pp. 774-781, 2012.

[44] C. J. Honey *et al.*, "Predicting human resting-state functional connectivity from structural connectivity," *Proc Natl Acad Sci U S A,* vol. 106, no. 6, pp. 2035-40, Feb 10 2009, doi: 10.1073/pnas.0811168106.

[45] G. L. Baum *et al.*, "Development of structure-function coupling in human brain networks during youth," *Proc Natl Acad Sci U S A,* vol. 117, no. 1, pp. 771-778, Jan 7 2020, doi: 10.1073/pnas.1912034117.

[46] D. Scheinost *et al.*, "Sex differences in normal age trajectories of functional brain networks," *Human brain mapping,* vol. 36, no. 4, pp. 1524-1535, 2015.

[47] J. J. Son *et al.*, "Developmental shifts in testosterone levels are associated with alterations in the neural oscillatory dynamics serving selective attention," *Imaging Neurosci (Camb),* vol. 3, 2025, doi: 10.1162/IMAG.a.120.

[48] G. Picci *et al.*, "Developmental changes in endogenous testosterone have sexually-dimorphic effects on spontaneous cortical dynamics," (in English), *Human Brain Mapping,* vol. 44, no. 17, pp. 6043-6054, Dec 1 2023, doi: 10.1002/hbm.26496.

[49] S. H. Penhale *et al.*, "Impacts of adrenarcheal DHEA levels on spontaneous cortical activity during development," *Dev Cogn Neurosci,* vol. 57, p. 101153, Oct 2022, doi: 10.1016/j.dcn.2022.101153.

[50] M. H. Fung *et al.*, "The impact of pubertal DHEA on the development of visuospatial oscillatory dynamics," *Hum Brain Mapp,* vol. 43, no. 17, pp. 5154-5166, Dec 1 2022, doi: 10.1002/hbm.25991.

[51] M. H. Fung *et al.*, "The development of sensorimotor cortical oscillations is mediated by pubertal testosterone," (in English), *Neuroimage,* vol. 264, Dec 1 2022, doi: ARTN e119745

10.1016/j.neuroimage.2022.119745.